Product Datasheet

YAP1 Antibody - BSA Free
NB110-58358

Unit Size: 0.1 ml

Aliquot and store at -20C or -80C. Avoid freeze-thaw cycles.

www.novusbio.com technical@novusbio.com

Reviews: 2 Publications: 79

Protocols, Publications, Related Products, Reviews, Research Tools and Images at:
www.novusbio.com/NB110-58358

Updated 5/21/2024 v.20.1

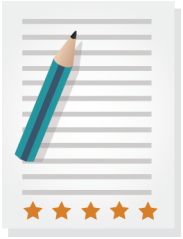

NB110-58358

YAP1 Antibody - BSA Free

Product Information	
Unit Size	0.1 ml
Concentration	1.0 mg/ml
Storage	Aliquot and store at -20C or -80C. Avoid freeze-thaw cycles.
Clonality	Polyclonal
Preservative	0.02% Sodium Azide
Isotype	IgG
Purity	Immunogen affinity purified
Buffer	PBS
Target Molecular Weight	48 kDa

Product Description	
Host	Rabbit
Gene ID	10413
Gene Symbol	YAP1
Species	Human, Mouse, Rat, Canine, Zebrafish
Reactivity Notes	Use in Human reported in scientific literature (PMID:33737385). Use in Zebrafish reported in scientific literature (PMID:28350986).
Specificity/Sensitivity	Expected reactivity based on immunogen homology: Isoform 4 (100%), Isoform 6 (100%)
Immunogen	This YAP1 Antibody was developed against a partial recombinant human YAP1 protein expressed in bacteria. [Uniprot: P46937], N-terminal GST fusion protein

Product Application Details	
Applications	Western Blot, Simple Western, Immunoblotting, Immunocytochemistry/ Immunofluorescence, Immunohistochemistry, Immunohistochemistry-Frozen, Immunohistochemistry-Paraffin, Immunoprecipitation, Chromatin Immunoprecipitation (ChIP), Knockdown Validated, Knockout Validated
Recommended Dilutions	Western Blot 1:1000, Simple Western 1:12.5, Immunohistochemistry 1:50-1:200, Immunocytochemistry/ Immunofluorescence, Immunoprecipitation 2-10 ug, Immunohistochemistry-Paraffin 1:50-1:200, Immunohistochemistry-Frozen reported in scientific literature (PMID 28581498), Immunoblotting reported in scientific literature (PMID 28406163), Chromatin Immunoprecipitation (ChIP), Knockout Validated, Knockdown Validated reported in scientific literature (PMID 28406163)
Application Notes	In Simple Western only 10 - 15 uL of the recommended dilution is used per data point. Separated by Size-Wes, Sally Sue/Peggy Sue.

Images

Immunocytochemistry/Immunofluorescence: YAP1 Antibody - BSA Free [NB110-58358] - Caco-2 cells were fixed in 4% paraformaldehyde for 10 minutes and permeabilized in 0.5% Triton X-100 in PBS for 5 minutes. The cells were incubated with YAP1 Antibody (NB110-58358) at 1 ug/ml overnight at 4C and detected with an anti-rabbit DyLight 488 (Green) at a 1:1000 dilution for 60 minutes. Nuclei were counterstained with DAPI (Blue). Cells were imaged using a 40X objective.

Western Blot: YAP1 Antibody - BSA Free [NB110-58358] - LW6 attenuates the accumulation of cellular YAP1 and its nuclear location. After treating PANC-1 cells with LW6 for 12 hours, LW6 decreased the accumulation of YAP1 when compared to Sham treated cells. n =5 per group. Image collected and cropped by CiteAb from the following publication (//pubmed.ncbi.nlm.nih.gov/31897243/) licensed under a CC-BY license.

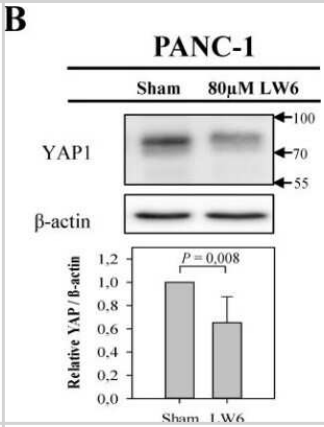

Immunocytochemistry/Immunofluorescence: YAP1 Antibody - BSA Free [NB110-58358] - YAP/TAZ signaling is not activated by loss of TRAF3. NT, NF2 KO1, and TRAF3 KO1 cells stained for YAP1 and DAPI. Image collected and cropped by CiteAb from the following publication (//pubmed.ncbi.nlm.nih.gov/33185187/) licensed under a CC-BY license.

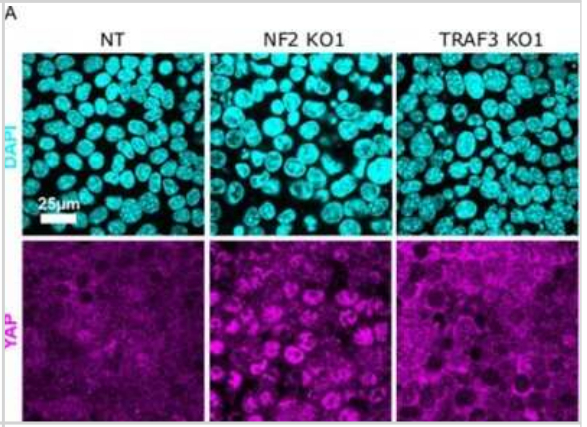

Immunohistochemistry-Paraffin: YAP1 Antibody - BSA Free [NB110-58358] - YAP1 was detected in immersion fixed paraffin-embedded sections of human placenta using Rabbit Anti-Human YAP1 polyclonal Antibody (Catalog # NB110-58358) at 1:200 for 1 hour at room temperature followed by incubation with the Anti-Rabbit IgG VisUCyte™ HRP Polymer Antibody (Catalog # VC003). Tissue was stained using DAB (brown) and counterstained with hematoxylin (blue). Specific staining was localized to nuclear and cytoplasm in trophoblast cells.

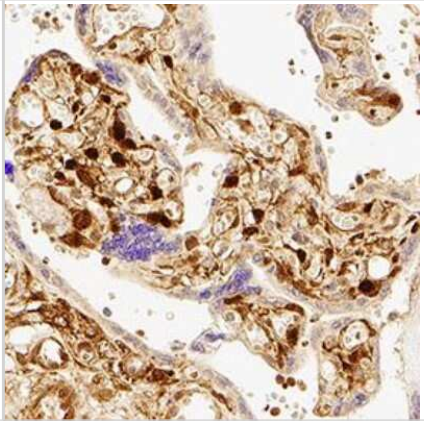

Western Blot: YAP1 Antibody - BSA Free [NB110-58358] - Analysis in transfected HEK 293 cell lysate using YAP1 antibody. Observed molecular weight 75 kDa.	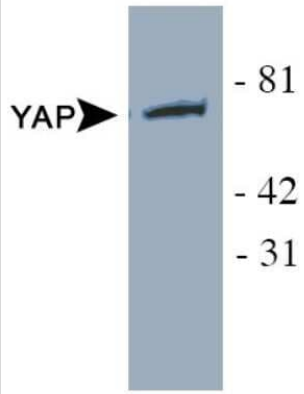
Western Blot: YAP1 Antibody - BSA Free [NB110-58358] - Consequences of ORP5 and ORP8 knockdown on downstream MAPK and PI3K/AKT signaling. Protein from MOH parental, single and double ORP knockdowns as well as cells transfected with empty vector control (pLKO.1) were harvested, and 20 ug was subjected to SDS-PAGE and used for Western blotting. Image collected and cropped by CiteAb from the following publication (https://www.life-science-alliance.org/lookup/doi/10.26508/lsa.201900431), licensed under a CC-BY license.	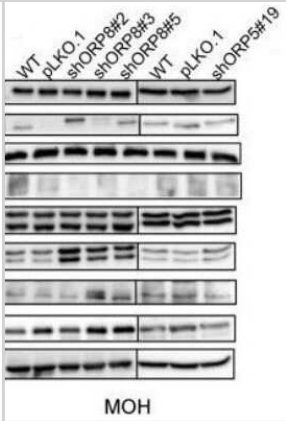
Western Blot: YAP1 Antibody - BSA Free [NB110-58358] - YAP1 Antibody [NB110-58358] - Actomyosin activity inhibits beta-catenin- and YAP-driven proliferation of confluent keratinocytes. Effects of cell density and actomyosin activity on YAP phosphorylation. HaCaT cells cultured for 40 h under the sparse and confluent conditions were treated with 100 uM blebbistatin (Blebb) or DMSO (for control) for 6 h, and then lysed and immunoblotted for Ser127-phosphorylated YAP (pYAP), YAP, beta-catenin and actin. Similar results were obtained in two independent experiments. Image collected and cropped by CiteAb from the following publication (https://www.nature.com/articles/srep46326), licensed under a CC-BY license.	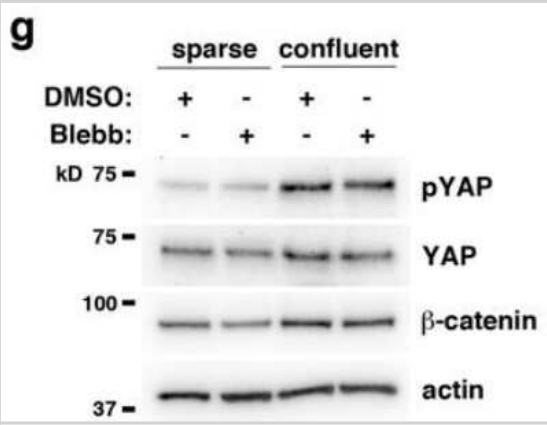
Simple Western: YAP1 Antibody - BSA Free [NB110-58358] - Simple Western lane view shows a specific band for YAP1 in 0.1 mg/ml of HeLa lysate. Observed molecular weight is 75 kDa. This experiment was performed under reducing conditions using the 12-230kDa separation system.	

Knockout Validated: YAP1 Antibody - BSA Free [NB110-58358] - Western blot shows lysates of HeLa human cervical epithelial carcinoma parental cell line and YAP1 knockout (KO) HeLa cell line. PVDF membrane was probed with 1:1000 of Rabbit Anti-Human YAP1 Polyclonal Antibody (Catalog # NB110-58358) followed by HRP-conjugated Anti-Rabbit IgG Secondary Antibody (Catalog #HAF008). Specific band was detected for YAP1 at approximately 75 kDa (as indicated) in the parental HeLa cell line, but is not detectable in the knockout HeLa cell line. This experiment was conducted under reducing conditions.	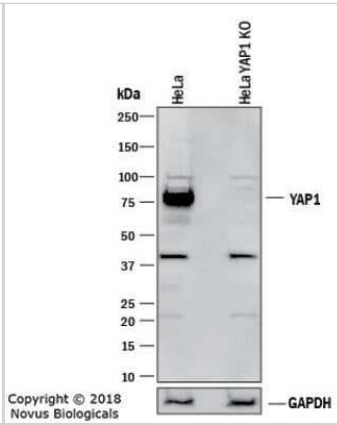
Knockout Validated: YAP1 Antibody - BSA Free [NB110-58358] - Western lane view shows lysates of HeLa human cervical epithelial carcinoma parental cell line and YAP1 knockout (KO) HeLa cell line. A specific band was detected for YAP1 at approximately 81 kDa (as indicated) using 50 ug/mL of Rabbit Anti-YAP1 Polyclonal Antibody (Catalog # NB110-58358). This experiment was conducted under reducing conditions and using the 12-230 kDa separation system.	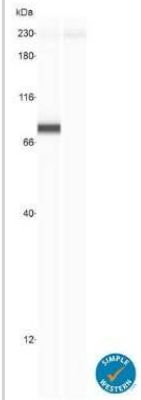
Actomyosin activity inhibits beta-catenin- and YAP-driven proliferation of confluent keratinocytes. (e and f) Confluent HaCaT cells cultured for 40 h were treated for 6 h with 100 uM blebbistatin (Blebb) or DMSO (for control) together with or without 75 uM iCRT3 (e) or 2 uM Verteporfin (VP) (f). The cells were then incubated with EdU for 2 h in the presence of the same combination of the drugs. The percentages of EdU positive cells are shown. *P < 0.005; **P < 0.001; N.S., no significant difference. n = 8 (>50 cells each) for each bar. Image collected and cropped by CiteAb from the following publication (https://www.nature.com/articles/srep46326), licensed under a CC-BY licence.	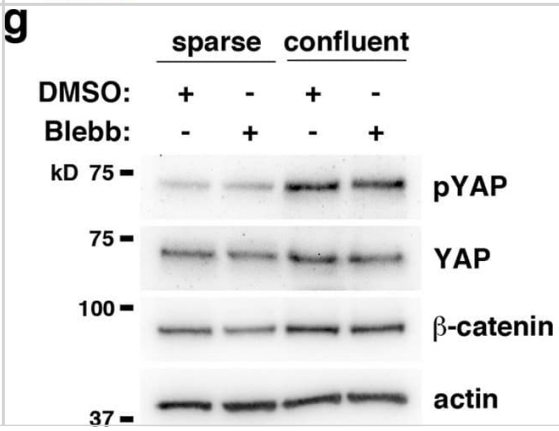

YAP and TAZ expression at high density and during chondrogenic differentiation of human synovial MSCs. (A) YAP and pYAP expression in human synovial membrane-derived (hSM-)MSCs in monolayer at low (L) and high (H) density detected by immunofluorescence staining, shown without (i) and with sytox green nuclear counterstain (ii). (B) YAP and pYAP expression in hSM-MSCs in monolayer at low (L) and high (H) density detected by western blotting with beta-actin as loading control. (C, D) Expression of YAP and TAZ (C) and their target genes CTGF and CYR61 (D) in hSM-MSCs immediately prior to (0 h) or 24 h after plating in micromass culture, determined by quantitative RT-PCR. Data was normalised to GAPDH expression, and is shown as mean +/- standard deviation (SD) (three donors) relative to pre-seeding (0 h) control. *P <0.05; **P <0.01; ***P <0.001. (E) Expression of YAP and TAZ in hSM-MSCs after 6 days of treatment with 10 ng/ml TGF-beta1 or vehicle only in micromass culture to induce chondrogenic differentiation, determined by quantitative RT-PCR. Data was normalised to GAPDH expression, and is shown as mean +/- SD (five donors) relative to vehicle-treated control. *P <0.05. (F) Detection of YAP by western blotting during chondrogenic differentiation induced by TGF-beta1 with detection of beta-actin as loading control. MSC, mesenchymal stromal/stem cell; pYAP, phosphorylated YAP; RT-PCR, reverse transcription PCR; TAZ, transcriptional co-activator with PDZ-binding motif; TGF, transforming growth factor; YAP, Yes-associated protein. Image collected and cropped by CiteAb from the following publication (https://pubmed.ncbi.nlm.nih.gov/26025096), licensed under a CC-BY licence.

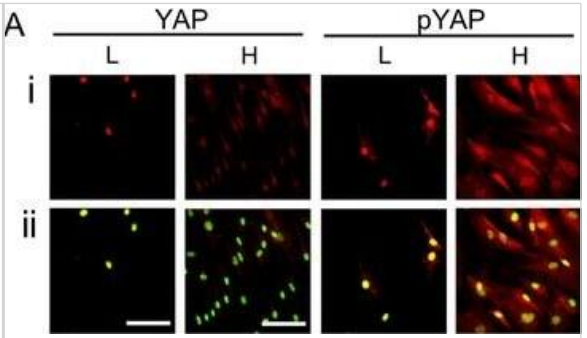

YAP/TAZ signaling is not activated by loss of TRAF3.(A) NT, NF2 KO1, and TRAF3 KO1 cells stained for YAP and DAPI. Image collected and cropped by CiteAb from the following publication (https://pubmed.ncbi.nlm.nih.gov/33185187), licensed under a CC-BY licence.

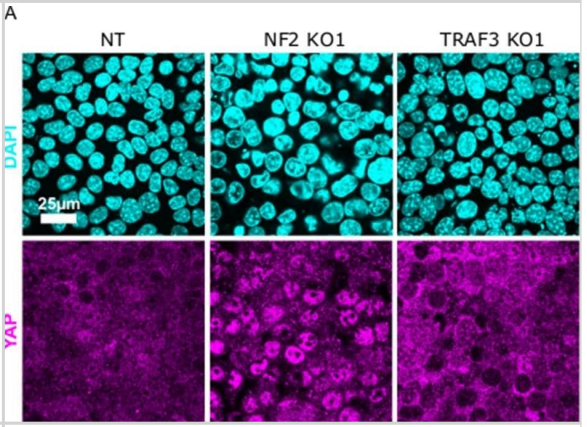

Ajuba depletion induces beta-catenin translocation and Cyclin D1 expression in HCC cell lines. a) Immunoblotting with specific antibodies against Ajuba, E-cadherin, beta-catenin, Cyclin D1, YAP, TAZ and CYR61 in Ajuba-depleted BEL7402 and HepG2 cells. GAPDH was used as a loading control. The ratios of expression E-Cadherin to their corresponding GAPDH are represented. Image collected and cropped by CiteAb from the following publication (https://pubmed.ncbi.nlm.nih.gov/30041665), licensed under a CC-BY licence.

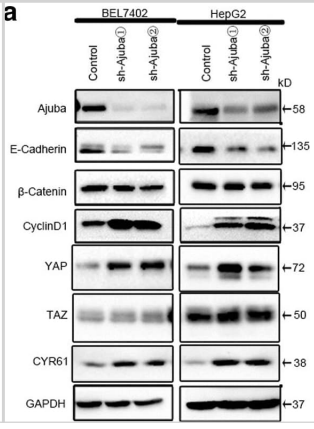

Consequences of ORP5 and ORP8 knockdown on downstream MAPK and PI3K/AKT signaling.Protein from BxPC-3, PANC-1, MiaPaCa-2, and MOH parental, single and double ORP knockdowns as well as cells transfected with empty vector control (pLKO.1) were harvested, and 20 ug was subjected to SDS-PAGE and used for Western blotting. EGFR, MAPK, and PI3K signaling were assayed as pEGFR, ppERK, and pAKT levels, respectively. Amplification of YAP-1 was also evaluated. Total ERK, total AKT, and beta-actin levels were used as loading controls. Image collected and cropped by CiteAb from the following publication (https://pubmed.ncbi.nlm.nih.gov/31451509), licensed under a CC-BY licence.	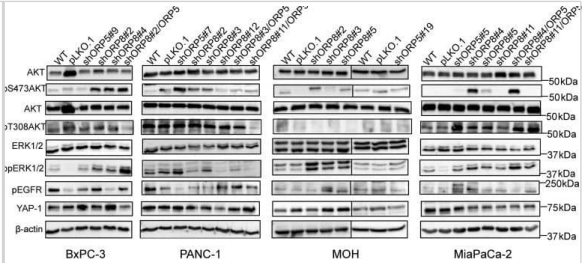
Fluorescence micrographs showing EGFR (Alexa 488; green), Rictor (Alexa 488; yellow) and cell nuclei (Hoechst 33342; blue) in GBM4 GBM-derived cancer stem-like cell line, and Gli36, U251MG, U118MG and LN229 GBM cell lines. Image collected and cropped by CiteAb from the following open publication (https://pubmed.ncbi.nlm.nih.gov/23555046), licensed under a CC-BY license. Not internally tested by Novus Biologicals.	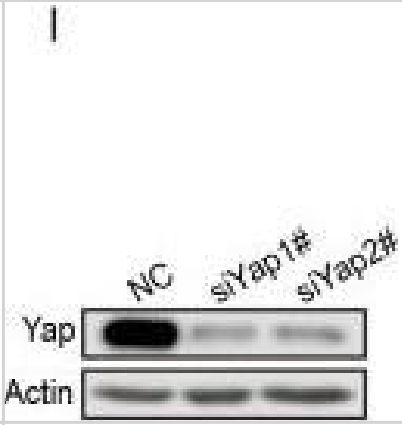
Xanthine Oxidase (XO) activity mediates HIF-2α degradation by IH. A–B Representative immunoblot of HIF-2α expression in cells exposed to IH in the presence of ALLO (A), and in cells transfected with XDH siRNA (B). C HIF-2α degradation in PC12cells treated with Xanthine (Xa)/XO (250 uM/0.01 U/ml) under normoxia, and the effect of MnTmPyP or ALLO co-treatment, respectively. Bottom panels of A, B and C show quantitative data of densitometric analysis presented as mean ± S.E.M. from 4 experiments, *p<0.05. n.s. not significant p>0.05. Image collected and cropped by CiteAb from the following open publication (https://pubmed.ncbi.nlm.nih.gov/24124516), licensed under a CC-BY license. Not internally tested by Novus Biologicals.	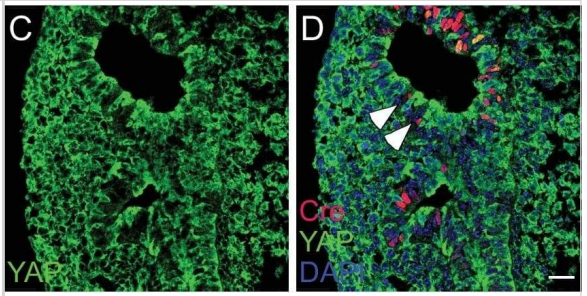
Effect of ET-1 on glucose uptake in HIF-1α-silenced astrocytes.Astrocytes were transfected with NT-siRNA or with HIF-1α-siRNA. After 48 h, astrocytes were incubated in the absence (control, C) or presence of 0.1 μM ET-1 for 24 h. A) HIF-1α, Hx-1, GLUT-3, Hx-2, GLUT-1 and GAPDH Western blots and quantification. The results are the means ± SEM of at least three independent experiments and they are expressed as percentages of the level found in the control NT-siRNA. B) Glucose uptake expressed as pmol of 2-deoxyglucose (2-DG) taken up per hour and per milligram of protein. The results show that the down-regulation of HIF-1α levels promoted by HIF-1α-siRNA decreased the rate of glucose uptake and the expression of GLUT-1, GLUT-3, Hx-1 and Hx-2, both in the control and in the ET-1 treated astrocytes. ***p<0.001, **p<0.01 and *p<0.05 versus the corresponding controls (C); ###p<0.001, ##p<0.01 and #p<0.05 versus the corresponding NT-siRNA. Image collected and cropped by CiteAb from the following open publication (https://dx.plos.org/10.1371/journal.pone.0032448), licensed under a CC-BY license. Not internally tested by Novus Biologicals.	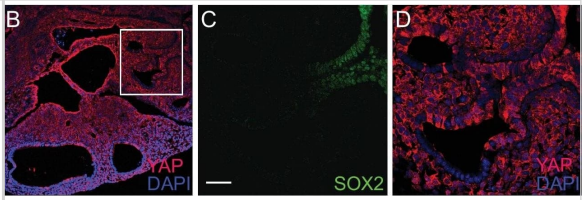

FKBP51 increases expression of melanoma CSC markers. (a) FKBP51 silencing decreases ABCB5 levels. (Left) Normalized expression rates (arbitrary units (AU)) (mean±S.D.) of FKBP51 (black) and ABCB5 mRNA (grey) (n=3). FKBP51-treated sample expression=1. (Right) Western blot assay of ABCB5 and FKBP51 levels. (b) FKBP51 overexpression enhances ABCB5 levels. (Left) Normalized expression of FKBP51 mRNA (black) and ABCB5 mRNA (grey) measured in WT, EV-, or FKBP51-stably transfected melanoma cells. WT sample expression=1; n=3. (Left) Western blot assay of ABCB5 and FKBP51 levels in the same cells. Anti-Flag-labelled exogenous FKBP51. (c) ABCG2+ melanoma cells increase in FKBP51-overexpressing cells. (Upper) Normalized expression of FKBP51 mRNA (black) and ABCG2 mRNA (grey) measured in WT, EV-, or FKBP51-stably transfected melanoma cells. WT sample expression=1; n=5. (Lower) Flow cytometric histograms of ABCG2 expression (green population); mean±S.D. of counts are shown. (d) Enhanced FKBP51 mRNA levels in sorted ABCG2+ melanoma cells (SAN, upper; A375, lower). Whole cell expression=1; (n=3). (e) Enhanced EMT gene transcripts in sorted ABCG2+ melanoma cells. ABCG2− sample expression=1; n=3. (f) Expression of ABCG2 transcript in 9 deparaffinized tumours, 4 primary melanoma (M) samples, and 5 metastases (MM). A naevus sample was arbitrarily chosen with expression=1 Image collected and cropped by CiteAb from the following open publication (https://www.nature.com/articles/cddis2013109), licensed under a CC-BY license. Not internally tested by Novus Biologicals.

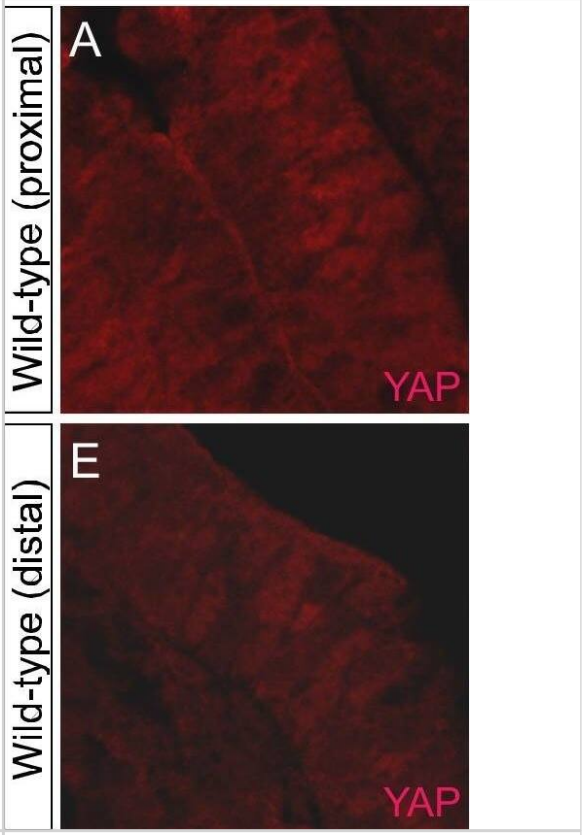

Tlk1-deficiency in mESCs causes a delay in the downregulation of core pluripotency factors upon differentiation. (A,C and E) Representative immunoblotting images showing Tlk1, Oct4, Sox2, and Nanog levels in Tlk1-KD cells upon differentiation. Differentiation was induced three different ways as previously described in Fig. 3. Alpha-tubulin was used as the loading control. (B,D and F) Quantification of the relative expression of the target proteins in panels (A,C, and E). The target proteins levels were normalized to that of α-tubulin. The protein expression levels of shLuc KD cells were normalized to 1. The biological data are presented as mean (n = 4) ± SEM for LIF- and EB and for RA (n = 3). *P < 0.05, **P < 0.01, and ***P < 0.001. (G) Immunofluorescence analysis of Oct4, Nanog and Tlk1 in control (shLuc) and Tlk1-deficient mESCs. Scale bars represent 100 μm. Image collected and cropped by CiteAb from the following open publication (https://pubmed.ncbi.nlm.nih.gov/29321513), licensed under a CC-BY license. Not internally tested by Novus Biologicals.

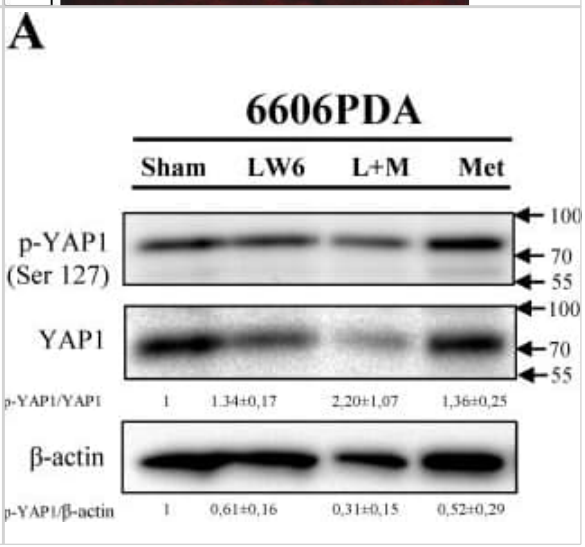

Publications

Enokido T, Horie M, Yoshino S et al. Distinct microRNA signature and suppression of ZFP36L1 define ASCL1-positive lung adenocarcinoma Molecular cancer research : MCR 2023-10-06 [PMID: 37801008]

Zhao X, Tang L, Le TP et al. Yap and Taz promote osteogenesis and prevent chondrogenesis in neural crest cells in vitro and in vivo Science Signaling 2022-10-25 [PMID: 36282910]

Xiao W, Pahlavanneshan M, Eun CY et al. Matrix stiffness mediates pancreatic cancer chemoresistance through induction of exosome hypersecretion in a cancer associated fibroblasts-tumor organoid biomimetic model Matrix Biology Plus 2022-06-01 [PMID: 35619988]

Moon S, Lee OH, Kim B et al. Estrogen Regulates the Expression and Localization of YAP in the Uterus of Mice International Journal of Molecular Sciences 2022-08-29 [PMID: 36077170] (ICC/IF, IHC)

McCourt JL, Stearns-Reider KM, Mamsa H et al. Multi-omics analysis of sarcospan overexpression in mdx skeletal muscle reveals compensatory remodeling of cytoskeleton-matrix interactions that promote mechanotransduction pathways Skeletal Muscle 2023-01-06 [PMID: 36609344] (ICC/IF, IHC-Fr)

Kastan N, Gnedeva K, Alisch T et al. Small-molecule inhibition of Lats kinases may promote Yap-dependent proliferation in postmitotic mammalian tissues Nature Communications 2021-05-25 [PMID: 34035288] (WB)

Sun X, Malandraki-Miller S, Kennedy T et al. The extracellular matrix protein agrin is essential for epicardial epithelial-to-mesenchymal transition during heart development Development 2021-05-01 [PMID: 33969874] (WB)

Wolfe AL, Zhou Q, Toska E et al. UDP-glucose pyrophosphorylase 2, a regulator of glycogen synthesis and glycosylation, is critical for pancreatic cancer growth Proceedings of the National Academy of Sciences 2021-08-03 [PMID: 34330832] (B/N)

Sunderland A, Williams J, Andreou T et al. Biglycan and reduced glycolysis are associated with breast cancer cell dormancy in the brain Frontiers in Oncology 2023-06-29 [PMID: 37456245] (ICC/IF)

Fetiva MC, Liss F, Gertzmann D et al. Oncogenic YAP mediates changes in chromatin accessibility and activity that drive cell cycle gene expression and cell migration Nucleic Acids Research 2023-05-22 [PMID: 36864753] (B/N)

Meliambro K, Yang Y, de Cos M et al. KIBRA upregulation increases susceptibility to glomerular injury and correlates with kidney function decline JCI insight 2023-02-28 [PMID: 36853804] (IHC-Fr, ICC/IF, Mouse, Human)

Karatsai O, Lehka L, Wojton D et al. Unconventional myosin VI in the heart: Involvement in cardiac dysfunction progressing with age Biochimica et biophysica acta. Molecular basis of disease 2023-05-09 [PMID: 37169038] (WB, Mouse)

More publications at http://www.novusbio.com/NB110-58358

Novus Biologicals USA
10730 E. Briarwood Avenue
Centennial, CO 80112
USA
Phone: 303.730.1950
Toll Free: 1.888.506.6887
Fax: 303.730.1966
nb-customerservice@bio-techne.com

Bio-Techne Canada
21 Canmotor Ave
Toronto, ON M8Z 4E6
Canada
Phone: 905.827.6400
Toll Free: 855.668.8722
Fax: 905.827.6402
canada.inquires@bio-techne.com

Bio-Techne Ltd
19 Barton Lane
Abingdon Science Park
Abingdon, OX14 3NB, United Kingdom
Phone: (44) (0) 1235 529449
Free Phone: 0800 37 34 15
Fax: (44) (0) 1235 533420
info.EMEA@bio-techne.com

General Contact Information
www.novusbio.com
Technical Support: nb-technical@bio-techne.com
Orders: nb-customerservice@bio-techne.com
General: novus@novusbio.com

Products Related to NB110-58358

NB820-59177	Human Brain Whole Tissue Lysate (Adult Whole Normal)
HAF008	Goat anti-Rabbit IgG Secondary Antibody [HRP]
NB7160	Goat anti-Rabbit IgG (H+L) Secondary Antibody [HRP]
NBP2-24891	Rabbit IgG Isotype Control

Limitations

This product is for research use only and is not approved for use in humans or in clinical diagnosis. Primary Antibodies are guaranteed for 1 year from date of receipt.

For more information on our 100% guarantee, please visit www.novusbio.com/guarantee

Earn gift cards/discounts by submitting a review: www.novusbio.com/reviews/submit/NB110-58358

Earn gift cards/discounts by submitting a publication using this product: www.novusbio.com/publications